



## GaN-Based LEDs Grown on HVPE Growth High Crystalline Quality Thick GaN Template

D. W. Lin,<sup>a</sup> C. C. Lin,<sup>b,z</sup> C. H. Chiu,<sup>a</sup> C. Y. Lee,<sup>a</sup> Y. Y. Yang,<sup>c</sup> Z. Y. Li,<sup>a</sup> W. C. Lai,<sup>c</sup> T. C. Lu,<sup>a</sup> H. C. Kuo,<sup>a,z</sup> and S. C. Wang<sup>a</sup>

<sup>a</sup>Department of Photonics and Institute of Electro-Optical Engineering, National Chiao Tung University, Hsinchu 300, Taiwan

<sup>b</sup>Institute of Photonic System, College of Photonics, National Chiao-Tung University, Guiren Township, Tainan County 71150, Taiwan

<sup>c</sup>Institute of Electro-Optical Science and Engineering, Cheng Kung University, Tainan 70101, Taiwan

In this study, high crystalline quality 30  $\mu\text{m}$  thick gallium nitride (GaN) films were grown by hydride vapor phase epitaxy (HVPE) on sapphire substrate, and the thick GaN films were used for developing high performance light-emitting diodes (LEDs). By using high-resolution X-ray diffraction, the full width at half-maximum (FWHM) of the rocking curve shows that this 30  $\mu\text{m}$  thick GaN template had high crystalline quality. In addition, the transmission electron microscopy (TEM) images suggest that threading dislocation densities (TDDs) are almost free in multiple quantum wells (MQWs) for LEDs grown on 30  $\mu\text{m}$  thick GaN template. Compared with conventional LEDs grown on sapphire, LEDs grown on 30  $\mu\text{m}$  thick GaN template exhibit 26% enhancement of light output at 20 mA.

© 2011 The Electrochemical Society. [DOI: 10.1149/2.003111jes] All rights reserved.

Manuscript submitted April 19, 2011; revised manuscript received July 13, 2011. Published October 5, 2011.

Nowadays, III-nitrides materials have attracted much attention and have been widely used in semiconductor devices, for both optoelectronics and electronics.<sup>1-3</sup> The III-nitride materials, including AlN, GaN, InN, and related alloys, cover a very wide range of direct bandgaps (From 0.7 to 6.1 eV). Such wide range of direct bandgap represents the emission wavelength from deep ultraviolet (UV) to infrared (IR) region. Nevertheless, up to now, GaN films are still grown on the foreign substrates, such as sapphire, GaAs, SiC, and silicon. Such heteroepitaxial layers typically show a high density of threading dislocations due to large lattice and thermal mismatches between GaN epilayers and substrates.<sup>4</sup> The threading dislocations (TDs) act as a non-radiative center inside GaN films and hence limit the light output efficiency of optoelectronic devices. To solve such problems, various growth techniques have been proposed to reduce the defect density and improve the crystalline quality, such as a low-temperature GaN buffer layer, multiple-step processes, high-temperature AlN buffer layers, and epitaxial lateral overgrowth (ELO).<sup>5,6</sup> On the other hand, the quantum-confined Stark effect (QCSE) caused by the internal piezoelectric field also plays an important role in light-emitting diodes (LEDs) devices performance. These effects may decrease the wave function overlap between holes and electrons and limit the output power of LEDs.<sup>7</sup>

In this work, we demonstrated InGaN-based LEDs grown on 30  $\mu\text{m}$ -thick GaN template. The 30  $\mu\text{m}$  thick GaN epilayers, which were grown on sapphire substrate by hydride vapor phase epitaxy (HVPE), show high crystalline quality and less strain. Compared to metal-organic chemical vapor deposition (MOCVD) and molecular beam epitaxy (MBE), the HVPE takes the advantages of higher growth rate,<sup>8</sup> which can reach several hundred micrometers per hour; as a result, it is one of the most suitable methods to grow thick bulk GaN to form freestanding substrates. We also grew the LED structures on this 30  $\mu\text{m}$  thick GaN template by MOCVD. The improvement of crystalline quality and strain relaxation effect of 30  $\mu\text{m}$  thick GaN template can help to greatly enhance the performance of LEDs. The optical and electrical characteristic of the LED devices grown on 30  $\mu\text{m}$  thick GaN template would also be analyzed and discussed in this work.

### Experimental

First of all, we will describe our wafer growth process. The 3  $\mu\text{m}$  thick GaN film was first grown by MOCVD on 2 inch c-plane

sapphire substrate. Then the 30  $\mu\text{m}$  thick GaN film was overgrown by HVPE in an Aixtron horizontal reactor. The chlorinated Ga and  $\text{NH}_3$  with a stream of  $\text{N}_2$  carrier gas were source materials for Ga and N, respectively. In the GaN growth process, the GaCl was obtained in a Ga source by reacting liquid gallium with HCl gas at 850°C. The V/III ratio was kept as a constant of 66.7. The HCl and  $\text{NH}_3$  flow rates were kept at 30 and 2000 sccm, respectively. The GaN buffer layer was deposited at temperature of 950°C and at pressure of 900 mbar for 4 minutes. After depositing the GaN buffer layer, the temperature was ramped to as high as 1050°C and the pressure was reduced to 300 mbar in 13 minutes and kept for 15 minutes for the growth of 30  $\mu\text{m}$  thick GaN epilayer.

The LED structures were grown on 30  $\mu\text{m}$  thick GaN templates with c-plane sapphire substrate by low pressure MOCVD system, as shown in Figure 1. The n-type GaN layer was doped with a concentration of  $3 \times 10^{18} \text{ cm}^{-3}$ . Then a ten-period InGaN/GaN MQW active layer was grown, consisting of 2 nm thick  $\text{In}_{0.22}\text{Ga}_{0.78}\text{N}$  wells and 12 nm thick GaN barriers. On the top of the active layer, there were 20 nm thick p- $\text{Al}_{0.1}\text{Ga}_{0.9}\text{N}$  electron blocking layer (EBL) and 0.2  $\mu\text{m}$  thick p-type GaN capping layer with a Mg doping concentration of  $1 \times 10^{20} \text{ cm}^{-3}$ . The corresponding hole concentration measured by Hall measurement was  $1 \times 10^{18} \text{ cm}^{-3}$ . Subsequently,  $350 \times 350 \mu\text{m}^2$  diode mesas were defined by chlorine-based reactive ion etching. Indium-tin-oxide (230nm) layer was used as the transparent p-contact and finally Cr/Au (100/250 nm) layers were deposited to be the p-GaN and n-GaN contact pads.

The strain in the 30  $\mu\text{m}$  thick GaN epilayers were analyzed by room temperature Raman measurements. High-resolution X-ray diffraction (HR-XRD) measurements rocking curves as  $\omega$  scans (0 0 2) and (1 0 2) were employed to investigate the crystalline quality of 30  $\mu\text{m}$  thick GaN films. In addition, transmission electron microscope (TEM) was carried out to analyze the threading dislocation densities (TDDs). The electronluminescent (EL) measurement was performed on probe station and the devices were probed on wafer directly, so light output was collected primarily on axial direction into the integrating sphere with a Si photodetector.

### Results and Discussion

To analyze the residual strain in the GaN films, Raman backscattering measurements were performed at room temperature. Figure 2 shows the Raman spectrum for 3  $\mu\text{m}$  and 30  $\mu\text{m}$  thick GaN epitaxial layer grown on sapphire substrate. The Raman shift peaks of  $E_2$  (high) mode for 3  $\mu\text{m}$  and 30  $\mu\text{m}$  thick GaN epitaxial layer are located at around 569.4 and 568.5  $\text{cm}^{-1}$ , respectively. Accordingly, the in-plane

<sup>z</sup> E-mail: chienchunglin@faculty.nctu.edu.tw; hckuo@faculty.nctu.edu.tw

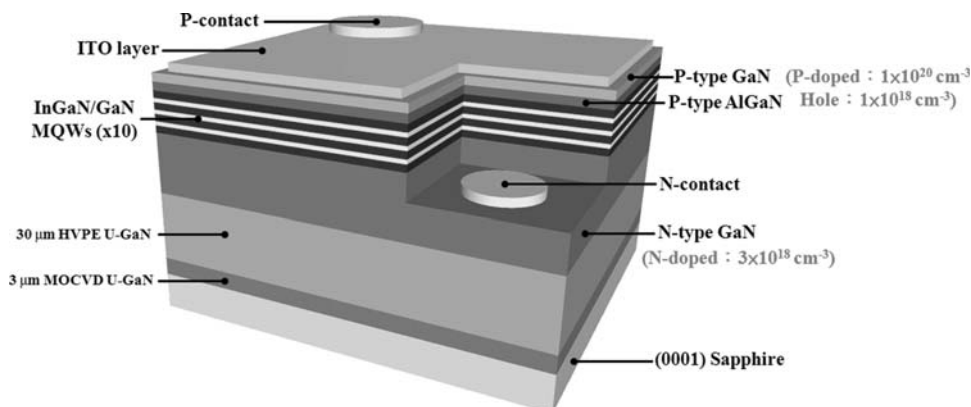


Figure 1. Schematic of GaN-based LED structures on 30- $\mu\text{m}$ -thick GaN template.

compressive stress  $\sigma$  for GaN epitaxial layer is estimated to drop from 1.28 GPa to 0.89 GPa with presence of thicker GaN epilayer, by using the following equation:<sup>9</sup>

$$\Delta\omega_{E_2} = \omega_{E_2} - \omega_0 = C\sigma \quad [1]$$

where  $\Delta\omega$  is the Raman shift peak difference between the strained GaN epitaxial layer  $\omega_{E_2}$  and the unstrained GaN epitaxial layer  $\omega_0$  ( $566.5 \text{ cm}^{-1}$ );  $C$  is the biaxial strain coefficient, which is  $2.25 \text{ cm}^{-1}/\text{GPa}$ . Consequently, we can expect that the GaN-based LED grown on such strain relaxation template have weaker QCSE.<sup>10</sup>

The X-ray diffraction (HR-XRD) rocking curves of both samples are shown in Fig. 3. The linewidth for (002) planes was reduced from 309 to 263 arc sec. The linewidth for (102) planes was reduced from 445 to 381 arc sec. The XRD linewidths for (102) and (002) planes are related to edge and screw threading dislocation densities, respectively.<sup>11</sup> The drop in XRD linewidth indicates improved material quality. These results indicated that the HVPE grown 30  $\mu\text{m}$  thick GaN had better crystalline quality than 3  $\mu\text{m}$  thick GaN grown by MOCVD. To analyze the detailed epitaxial layer quality, we used TEM to compare the cross section between two types of devices.

Figure 4 shows TEM images of LED structures grown on 30  $\mu\text{m}$  thick GaN templates. As we can see from Fig. 4a, few TDs are observed in the regions of 30  $\mu\text{m}$  HVPE grown GaN epilayers. For estimating the quantity of threading dislocation density in 30  $\mu\text{m}$  HVPE grown GaN epilayers precisely, the technique of etching pit

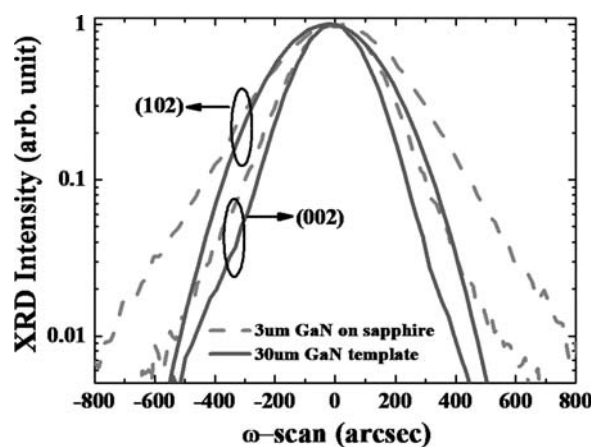


Figure 3. HR-XRD rocking curves for 3  $\mu\text{m}$  and 30  $\mu\text{m}$  thick GaN epitaxial layer.

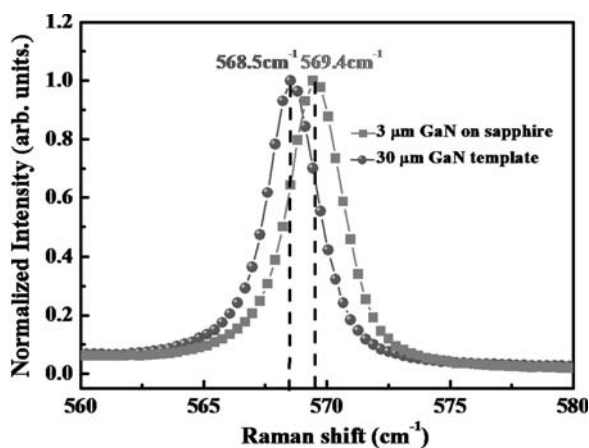


Figure 2. Raman spectrum for 3  $\mu\text{m}$  and 30  $\mu\text{m}$  thick GaN epitaxial layer.

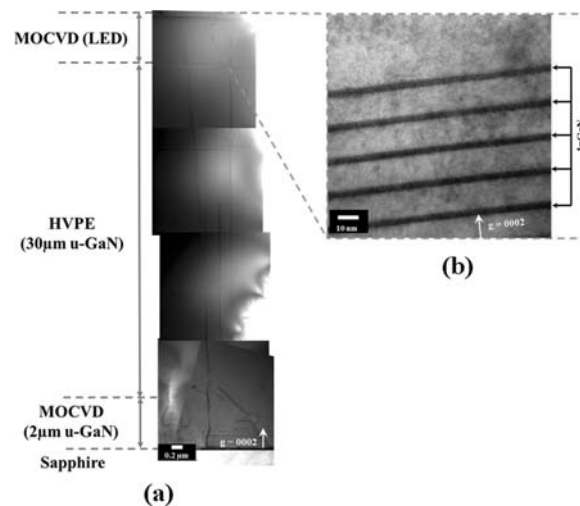
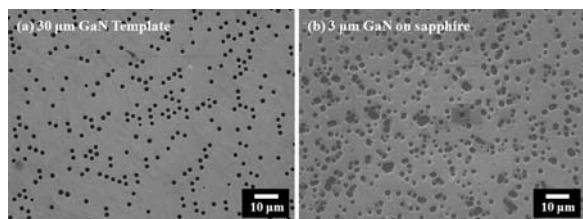


Figure 4. (a) TEM image of GaN-based LED structures on 30- $\mu\text{m}$ -thick GaN template; (b) a magnified view of (a). The diffraction condition is  $g = 0002$ .



**Figure 5.** Top view SEM images of etching pit density (EPD) pattern for (a) 30  $\mu\text{m}$  GaN Template and (b) 3  $\mu\text{m}$  GaN on sapphire.

density (EPD) pattern performed at 300 °C for 1 min by KOH solution was employed. Figure 5a and 5b show the top view SEM images of EPD pattern for 30  $\mu\text{m}$  GaN template and 3  $\mu\text{m}$  GaN on sapphire, respectively. The corresponding etching pits were estimated to about  $3 \times 10^6 \text{ cm}^{-2}$  for 30  $\mu\text{m}$  thick GaN template, which was less than the etching pits for 3  $\mu\text{m}$  GaN on sapphire (more than  $10^8 \text{ cm}^{-2}$ ). The reduction of etching pits was correlated to threading dislocation density directly. The reduction of etching pits and TDDs can be attributed to better crystalline quality of thick GaN epilayers provided by HVPE and less residual strain caused by gradually strain relaxation through the thick GaN growth technique. On the other hand, it has been reported that strain in the MQWs and In distribution inhomogeneities in the InGaN well are the main factors responsible for the V-defect occurrence and propagation.<sup>12,13</sup> As discussed above, for the LED on HVPE grown 30  $\mu\text{m}$  thick GaN epilayer, the strain in the MQWs is relatively small. However, from the cross-section high resolution TEM (HRTEM) image in Fig. 4b, one can clearly observe certain well width and composition fluctuations in MQW layer. These may not only induce additional V-defects but also influence the subsequent growth of the MQWs layer.

LED devices with a chip size of  $350 \times 350 \mu\text{m}^2$  were then fabricated from the completed epitaxial structures. Figure 6a shows the typical power-current-voltage (L-I-V) characteristics of both samples. With an injection current of 20 mA, the forward voltages are 3.37 and 3.47 V, and the output powers are 20.1 and 15.8 mW, respectively. At 20 mA, the light output power of the LED on HVPE grown 30  $\mu\text{m}$  thick GaN epilayer was 26% higher than that of the LED on 3  $\mu\text{m}$  thick GaN template. The better L-I-V characteristics can be attributed to the TDDs reduction of epitaxial layers. This reduction leads to much fewer non-radiative recombination events and less current leakage path in the 30  $\mu\text{m}$  thick GaN template. It's well known that LED with fewer non-radiative recombination centers and less current leakage path could efficiently reduce the forward voltage and increase the photon generation efficiency. Figure 6b displays EL emission peak wavelength as a function of injection current for two samples. The emission peak wavelength of LED grown on 30  $\mu\text{m}$  HVPE GaN template is slightly red-shifted (about 3.3 nm) from that of LED grown on 3  $\mu\text{m}$  MOCVD GaN epilayer, and this is reasonable since lateral strain

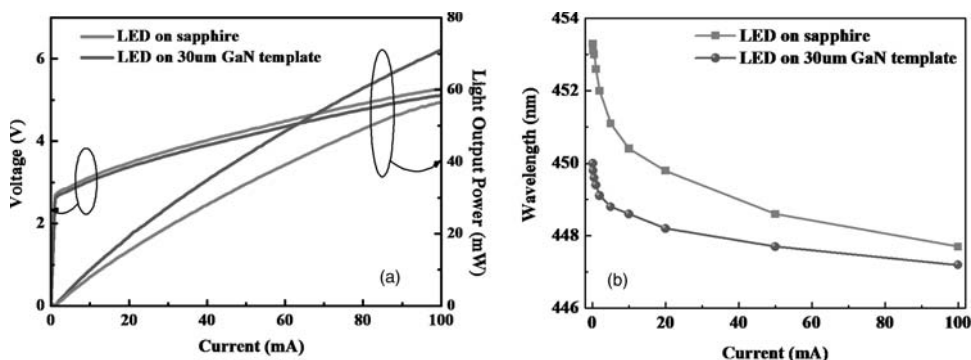


**Figure 6.** (a) L-I-V characteristics of the two fabricated LEDs. (b) The EL peak wavelength as a function of injection current of two fabricated LEDs.

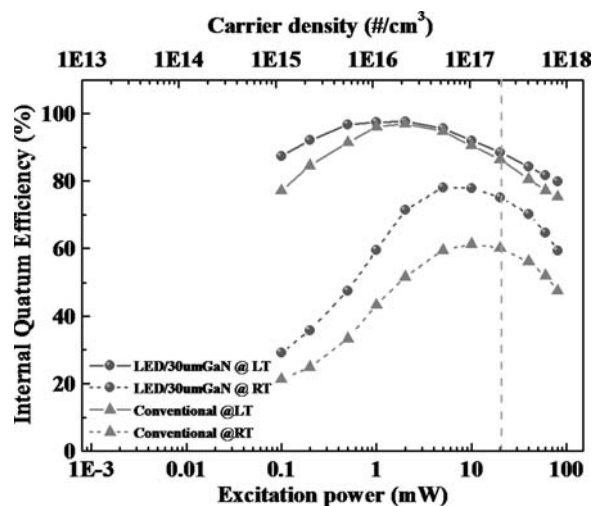


**Figure 7.** Relative internal quantum efficiency as a function of excitation power for two fabricated LEDs.

relaxation favors higher indium incorporation.<sup>14-16</sup> More importantly, as we increase the injection current, the emission peak wavelength of LED grown on 30  $\mu\text{m}$  HVPE GaN template exhibits smaller blueshift (around 2.8 nm) compared with that of LED grown on 3  $\mu\text{m}$  MOCVD GaN epilayer (around 5.6 nm). This result indicates that the QCSE does become weaker due to the strain relaxation in epitaxial layer overgrown on 30  $\mu\text{m}$  thick GaN template.<sup>17</sup>

In order to confirm the efficiency improvement of LED grown on 30  $\mu\text{m}$  HVPE GaN template, the PL internal quantum efficiency (IQE) measurement was performed. A general approach to evaluate the IQE of LEDs is to compare the PL integrated intensity between low and room temperatures.<sup>18</sup> A general assumption of this method is that the measured quantum efficiency at low temperature is free from non-radiative recombination loss and thus the injected carriers are almost 100% contributed to light-emitting processes. Figure 7 shows the measured IQE as a function of excitation power at 15 K and 300 K for both samples. The efficiency is defined as the collected photon numbers divided by the injected photon numbers and normalized to the maximum efficiency at low temperature.<sup>19</sup> At 20 mW of excitation power, it can be found that the IQE increase from 60% (conventional LEDs) to 72% (LEDs grown on 30  $\mu\text{m}$  thick GaN template), which corresponds to 1.25 times enhancement of efficiency. At this excitation level, we could calculate the corresponding generated carrier density to be  $2 \times 10^{17} \text{ cm}^{-3}$ , approximately same level of 20 mA at room temperature in our device. Compared with the L-I-V measurement, we can see closely-matched EQE enhancement (26% at 20 mA) from actual device. Since we didn't include any light-extraction mechanism in both reference and HVPE samples, we

believe the improvement shall be attributed solely to the IQE increase due to better material quality in HVPE samples. The efficiency improvement of LED on HVPE grown 30- $\mu\text{m}$ -thick GaN epilayer can be linked directly to the improvement of IQE due to better crystal quality.

### Conclusion

In summary, we demonstrated high crystalline quality 30  $\mu\text{m}$  thick GaN template grown by HVPE on sapphire substrate, and the thick GaN films were used for developing high performance LEDs. From Raman measurement, it was found that the residual stress was reduced from 1.28 GPa to 0.89 GPa in GaN epitaxial layer using 30  $\mu\text{m}$  thick GaN template. By using high-resolution X-ray diffraction, the narrow full width at half-maximum of the rocking curve indicates good crystalline quality of this 30  $\mu\text{m}$  thick GaN template. In addition, the transmission electron microscopy (TEM) images suggest that threading dislocation densities (TDDs) are almost free in multiple quantum wells (MQWs) for LEDs grown on 30  $\mu\text{m}$  thick GaN template. Compared with conventional LEDs grown on sapphire, LEDs grown on 30  $\mu\text{m}$  thick GaN template exhibit smaller EL peak wavelength blue shift and great enhancement of the light output (26% at 20mA), and this is close to what we observed in IQE measurement (25%). Thus, it is conceivable that 30  $\mu\text{m}$  thick GaN template can achieve better LEDs performance by lower TDs, strain relaxation and weaker QCSE.

### Acknowledgments

The authors are grateful to the National Science Council of the Republic of China, Taiwan, for financially supporting this research under Contract No. NSC 98-3114-E-009-002-CC2. We also greatly thank NAMIKI PRECISION JEWEL co., LTD. and Mr. Koyama Koji for technical support.

### References

1. S. Nakamura, M. Senoh, N. Iwasa, T. Yamada, T. Matsushita, H. Kiyoku, Y. Sugimoto, T. Kozaki, H. Umemoto, M. Sano, and K. Chocho, *Jpn. J. Appl. Phys.*, **36**, 1586 (1997).
2. S. Keller, R. Vetury, G. Parish, S. P. DenBaars, and U. K. Mishra, *Appl. Phys. Lett.*, **78**, 3088 (2001).
3. Y. Narukawa, I. Niki, K. Izuno, M. Yamada, Y. Murazki, and T. Mukai, *Jpn. J. Appl. Phys.*, **41**, 371 (2002).
4. S. Nakamura, M. Senoh, S. Nagahama, N. Iwasa, T. Yamada, T. Matsushita, H. Kiyoku, Y. Sugimoto, T. Kozaki, H. Umemoto, M. Sano, and K. Chocho, *Appl. Phys. Lett.*, **72**, 211 (1998).
5. D. Kapolnek, S. Keller, R. Vetury, R. D. Underwood, P. Kozodoy, S. P. Den Baars, and U. K. Mishra, *Appl. Phys. Lett.*, **71**, 1204 (1997).
6. Tsvetankov S. Zheleva, Ok-Hyun Nam, Michael D. Bremser, and Robert F. Davis, *Appl. Phys. Lett.*, **71**, 2472 (1997).
7. S. H. Park, *J. Appl. Phys.*, **91**, 9904 (2002).
8. C. E. C. Dam, A. P. Grzegorzczak, P. R. Hageman, R. Dorsman, C. R. Kleijn, and P. K. Larsen, *J. Crystal Growth*, **271**, 192 (2007).
9. P. Puech, F. Demangeot, J. Frandon, C. Pinquier, M. Kuball, V. Domnich, and Y. Gogotsi, *J. Appl. Phys.*, **96**, 2853 (2004).
10. C. H. Chiu, Zhen-Yu Li, C. L. Chao, M. H. Lo, H. C. Kuo, P. C. Yu, T. C. Lu, S. C. Wang, K. M. Lau, and S. J. Cheng, *J. Crystal Growth*, **310**, 5170 (2008).
11. H. Heinke, V. Kirchner, S. Einfeldt, and D. Hommel, *Appl. Phys. Lett.*, **77**, 2145 (2000).
12. I. H. Kim, H. S. Park, Y. J. Park, and T. Kim, *Appl. Phys. Lett.*, **73**, 1634 (1998).
13. D. I. Florescu, S. M. Ting, J. C. Ramer, D. S. Lee, V. N. Merai, A. Parkeh, D. Lu, E. A. Armour, and L. Chernyak, *Appl. Phys. Lett.*, **83**, 33 (2003).
14. K. Y. Zang, Y. D. Wang, H. F. Liu and S. J. Chua, *Appl. Phys. Lett.*, **89**, 171921 (2006).
15. A. Kikuchi, M. Kawai, M. Tada, and K. Kishino, *Jpn. J. Appl. Phys.*, **43**, 1524 (2004).
16. A. Kikuchi, M. Tada, K. Miwa, and K. Kishino, *Proc. SPIE*, **6129**, 612905 (2006).
17. C. H. Chiu, P. M. Tu, C. C. Lin, D. W. Lin, Z. Y. Li, K. L. Chuang, J. R. Chang, T. C. Lu, H. W. Zan, C. Y. Chen, H. C. Kuo, S. C. Wang, and C. Y. Chang, *IEEE J. Sel. Topics Quantum Electron*, **10**, 1109 (2010).
18. S. Watanabe, N. Yamada, M. Nagashima, Y. Ueki, C. Sasaki, Y. Tamada, T. Taguchi, and H. Kudo, *Appl. Phys. Lett.*, **83**, 4906 (2003).
19. Y. J. Lee, C. H. Chiu, C. C. Ke, P. C. Lin, T. C. Lu, H. C. Kuo, and S. C. Wang, *IEEE J. Sel. Topics Quantum Electron*, **15**, 1137 (2009).